Dynamic Covalent Synthesis Applied to Optoelectronic and Energy Materials: Design, Applications and Limitations

Elarbi Chatir, Arthur H G David, Adèle Gapin, Antoine Goujon

EurJOC
European Journal of Organic Chemistry

Chemistry Europe
European Chemical Societies Publishing

Accepted Article

Title: Dynamic Covalent Synthesis Applied to Optoelectronic and Energy Materials: Design, Applications and Limitations

Authors: Elarbi Chatir, Arthur David, Adèle Gapin, and Antoine Goujon

To be cited as: *Eur. J. Org. Chem.* **2024**, e202400211

Link to VoR: https://doi.org/10.1002/ejoc.202400211

WILEY VCH

10.1002/ejoc.202400211

WILEY VCH

REVIEW

Dynamic Covalent Synthesis Applied to Optoelectronic and Energy Materials: Design, Applications and Limitations

Elarbi Chatir,[a]† Arthur H. G. David,[a]† Adèle Gapin[a]† and Antoine Goujon*[a]

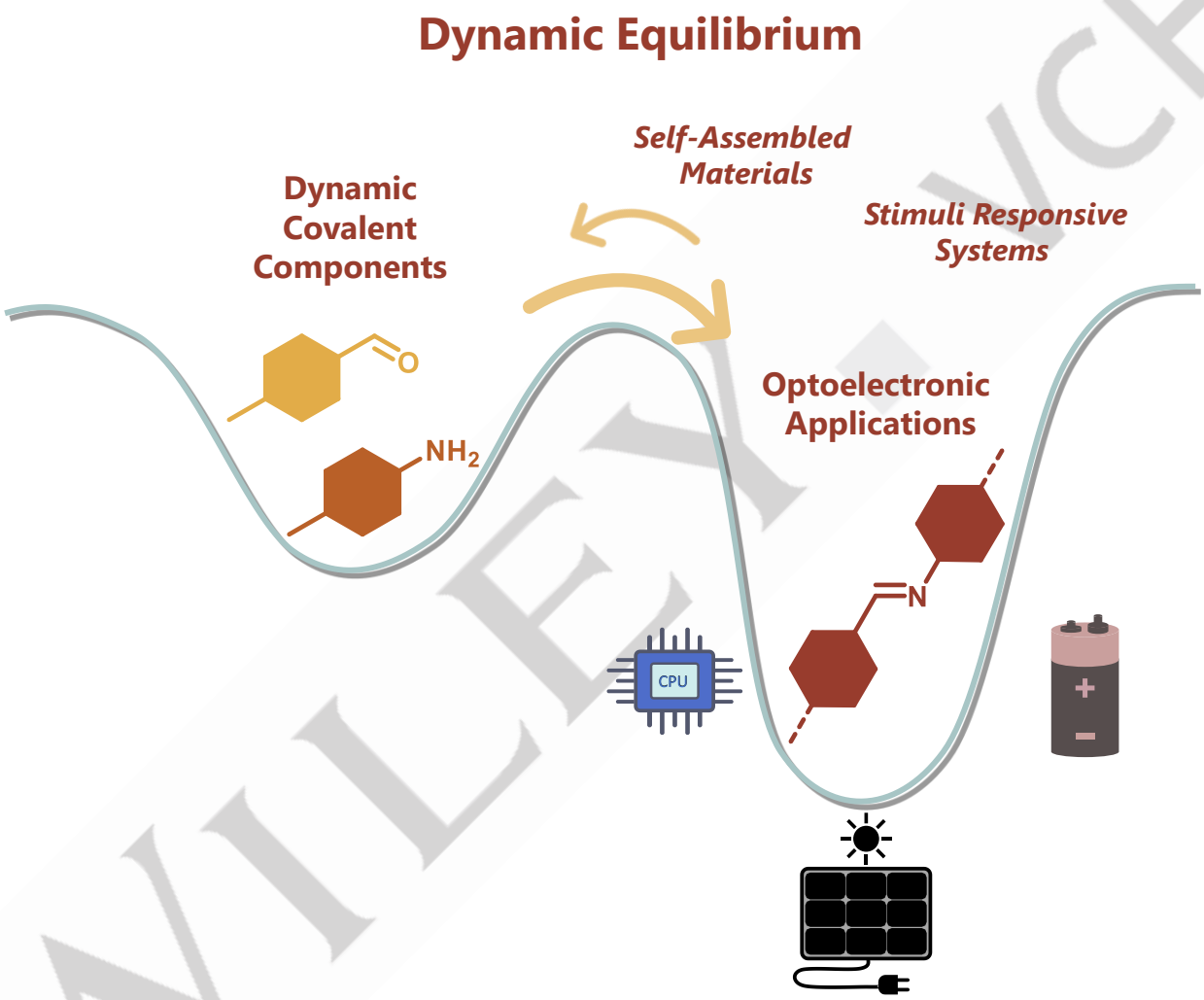

10.1002/ejoc.202400211

WILEY VCH

REVIEW

[a] Dr. A. Gapin, Dr. A. H. G. David, Dr. E. Chatir, Dr. A. Goujon
Univ Angers, CNRS, MOLTECH-Anjou, SFR MATRIX
49000 Angers (France)
E-mail: antoine.goujon@univ-angers.fr
† E. Chatir, A. H. G. David and A. Gapin contributed equally and were placed in alphabetical order.

Abstract: Dynamic Covalent Chemistry, consisting in the use of dynamic covalent bonds (DCBs) to create complex objects by working at the thermodynamic equilibrium, has undeniable advantages for the preparation of conjugated systems with tailored optoelectronic properties for organic electronics. Chemists can combine simple building blocks with simple functional groups of appropriate geometry, structure and stoichiometry to build multidimensional conjugated architectures. Dynamic covalent reactions are often precious metal-free, generate little to no side products and are very efficient. DCBs however afford sensitive materials, and consequently a balance needs to be found between the ease of synthesis, the stability and the performances. The dynamicity of the target materials hence can considerably reduce their applicability in organic electronics where strongly stable materials are needed, but opens the door to stimuli-responsive behaviour and recyclability. A way to overcome dynamicity issues is to lock DCBs, but often at the cost of decreased conjugation. In this review, we will highlight how DCBs are employed to prepare functional optoelectronically active materials, such as discrete molecules, polymers or covalent organic frameworks, applied in fields ranging from organic light-emitting diodes and solar cells to organic batteries and transistors. We will also discuss their limitations, benefits and the current challenges to overcome.

1. Introduction

Dynamic covalent chemistry (DCC) involves the reversible formation of covalent bonds as a molecular engineering strategy.[1–4] Common dynamic covalent bonds (DCBs) include imines, esters, disulfides, alkynes (in presence of a catalyst), boronic esters, or sometimes heteroatoms linked to aromatic scaffolds.[5] The particularity of DCBs is that, in the right conditions, systems bearing DCBs can disassociate back to their starting materials: DCBs are continuously forming, separating and re-attaching at different rates and are characterized by a highly tunable thermodynamic equilibrium that can be easily adjusted by altering the reaction parameters (temperature, solvent, acidity, *etc.*) and the nature of the reactants.[6–8] Moreover, DCBs are often orthogonal and offer the possibility to simultaneously assemble and set in motions different components.[9–12] This dynamicity presents undeniable advantages for the synthesis of new materials being constructed by template-assisted self-assembly, and/or featuring self-correction, self-sorting and adaptation properties.[13–15]

Compared to regular kinetically irreversible stepwise synthesis, DCC allows chemists to produce complex molecular architectures which would be difficult or impossible to reach in a single synthetic step by selecting appropriate buildings blocks and reacting them in a precise environment in a specific stoichiometry. DCC has been used with great success in various fields, cementing its role as an advantageous synthetic tool. As we were writing this manuscript, Cougnon, Stefankiewicz and Ulrich published a very insightful review detailing how DCC can now be used to address specific synthetic challenges and access a wide variety of structures and functions *via* dynamic covalent synthesis.[16] They also warn of kinetic biases, which sometimes might direct the formation of a major compound against the thermodynamic one. In consequence, attempts at self-assembling sub-components into complex architectures thanks to DCBs can sometimes lead to an unpredictable outcome. That being said, they insist on the advantages of such strategies and invite chemists to seize the limitless potential of DCC.

In the field of organic electronics or energy-related materials, DCBs can be used to combine simple π-conjugated components with complementary optoelectronic properties together and (self-)assemble them into complex conjugated systems. Moreover, the functional groups involved in these reactions are usually easy to install on a wide variety of aromatic scaffolds and circumvent the use of toxic or precious metals. This methodology is particularly attracting considering that the development of new active components for organic electronic devices is blooming.[17] Tailored conjugated systems are required to push the performances of organic solar cells, transistors or light-emitting devices. Organic semiconductors are also present in high-performances batteries, supercapacitors and thermoelectric conversion devices. It is essential to highlight that low-energy consuming, easy to process and cheap to produce organic electronics will contribute to support a more sustainable future where efficient and low-carbon emitting energy production/storage technology will be crucial.

Although DCC synthetic strategies possess many advantages, they have been relatively underrepresented in the syntheses of electronically active materials, except for covalent organic frameworks (COFs) in which DCBs are ubiquitous:[18] their dynamic character is required in this case to produce crystalline materials. Additionally, introducing dynamic and reversible bonds in π-conjugated materials can give them peculiar stimuli-responsiveness, multifunctional properties, or turn them recyclable/degradable.

In this non-exhaustive review, we will discuss the use of DCC and DCBs in optoelectronic materials. DCBs can be used to organize or self-assemble chromophores in space without direct conjugation, or link them together in a more or less dynamic fashion. This dynamic character becomes sometimes an important feature of the final material, nonetheless, it can sometimes hamper its stability or performances. We will illustrate these problematics by focussing either on specific kinds of DCB, or on specific fields exploiting DCBs. After discussing selected relevant examples of discrete compounds, polymers or COFs, we will highlight the limitations and strengths of this approach, while discussing potential future developments.

10.1002/ejoc.202400211

Dr. Adèle Gapin obtained her PhD degree in Polymer Chemistry from the University of Pau in 2020, working on the elaboration of functional copolymers absorbing in the near infrared region. In 2021, she joined the Sustainable Polymer Chemistry group at the University of Twente to work on the synthesis of biodegradable polymers, in close collaboration with BASF SE. In 2022, she worked on the visible-light driven synthesis of semi-conducting polymers at the Moltech-Anjou laboratory alongside Dr. Antoine Goujon. She now works on developing biodegradable semi-conducting polymers for optoelectronic and bioelectronic applications as Assistant Professor at the LCPO/University of Bordeaux.

Dr. Arthur H. G. David received his Ph.D. from the University of Granada, Spain, under the supervision of Drs. Victor Blanco and Araceli G. Campaña, working on rotaxanes and heptagon-containing nanographenes. He moved to Northwestern University, USA, to join Prof. J. Fraser Stoddart's group where he worked on luminescent pumps, cyclophanes, and catenanes. He pursued his carrier with Dr. Antoine Goujon at the University of Angers, France, studying electron-poor nanographenes for organic electronics. Currently, Arthur is a postdoctoral researcher at the same University, in Dr. Philippe Blanchard's group. His research is centered on the synthesis of chromophores for organic photovoltaics.

Elarbi Chatir received his Master degree in organic chemistry from the university of Grenoble Alpes in Grenoble in 2019. The same year, he starts his Ph.D. under the supervision of Dr. Saioa Cobo at the University of Grenoble Alpes. His research focuses on the development and study of photo and electro-switchable molecular materials based on dithienylethene derivatives. His current research focuses on the design and synthesis of novel conjugated semiconducting materials.

Antoine Goujon is an Associate Professor in the MOLTECH-Anjou Laboratory at the University of Angers, France, since 2019. He obtained his PhD in 2016 from the lab of Prof. Nicolas Giuseppone at the University of Strasbourg and performed his postdoctoral research in the group of Prof. Stefan Matile in Geneva. His research interests range from supramolecular chemistry to organic materials and semiconductors. He recently received the Marc Julia "Emergent Scientist" Award from the Organic Chemistry Division of the French Chemical Society, and was awarded an ERC Starting Grant in 2023 to develop dynamic covalent approaches for organic semiconductors synthesis.

2. DCC as a Tool to Self-Assemble or Organize Opto-Electroactive Architectures in Space

DCC can be used to precisely assemble opto-electroactive units in space so that complex functions emerge from simple building blocks. The orthogonality between different DCBs is here playing a central role in the creation of functional multichromophoric architectures. Two representative examples of this approach are the light-harvesting antennas reported by the groups of Bonifazi[19] and Matile.[20] Bonifazi and co-workers reported helical peptides backbones incorporating modified amino-acids decorated with functional groups, precursors of DCBs such as disulfides, hydrazides and diols (**Figure 1a**).[21] Chromophores with orthogonal groups (thiols, aldehydes and boronic acids) were attached to the peptide, precisely organizing them in space around its α-helix. The result is an antenna absorbing light all-across the visible range in which excitation of one dye triggers an energy cascade reminiscent of what happens in biological photosynthetic systems. Matile and co-workers functionalized naphthalene diimides (NDIs) with disulfides to self-assemble charge-transporting channels perpendicularly to a surface following a self-organizing surface-initiated polymerization approach (**Figure 1b**).[22] These NDIs were laterally decorated with a hydrazide group which was later reacted with different aldehyde-functionalized NDIs to create additional parallel channels. By adjusting the energy levels of the chromophore, *i.e.* tuning their core-functionalization, distinct n-type and p-type channels emerge leading to the bottom-up fabrication of a well-defined heterojunction. Photocurrent was indeed observed under exposure to a solar simulator. These systems were greatly complexified in following work, with the introduction of a third component and the use of more diverse dyes and organic semiconductors.[23–25] These elegant and sophisticated examples illustrate the powerful organizational power that orthogonal DCBs offer and how it can be used to mimic photosynthetic processes. In these works, DCBs are used to precisely assemble conjugated systems in space but not to strictly establish a covalent electronic conjugation between them or extend the size of a conjugated system. The final functional architectures do not further exploit the reversible character of the DCBs.

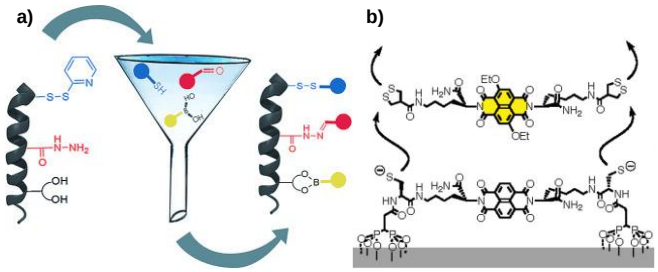

Figure 1. a) Orthogonal dynamic covalent self-assembly of chromophores along a peptide backbone.[21] b) Self-organizing surface-initiated polymerization used for the fabrication of artificial photosystems.[22] Reprinted with permission from ref. [21]. Copyright 2015 Wiley-VCH. Reprinted with permission from ref. [22]. Copyright 2011 American Chemical Society.

10.1002/ejoc.202400211

3. Discrete DCBs-Containing Materials Used in Optical and/or Electronic Materials or Devices

3.1 Imine Bonds or Schiff Bases

The reaction between amines and aldehydes stands as one of the most commonly used reactions in DCC. The formation of an imine bond[26] is a rapid and efficient process involving an amine (NH_2) and a carbonyl group (C=O) reacting to form a carbon-nitrogen double bond (C=N).[27] Several external factors including temperature, solvent, concentration and pH affect the equilibrium between an imine and its starting materials. Imines commonly participate to other reactions under thermodynamic equilibrium:[28] (i) amine exchanges which consist in the addition of another amine replacing the original one and therefore leading to transamination, and (ii) metathesis reactions in which the addition of a second imine causes a scrambling between the different subcomponents. There are only few electronically active and relevant discrete compounds incorporating imines that have been tested in devices. We have selected a few examples below to illustrate this chemistry and its possibilities in several applications.

3.1.1 Proton Conductivity

Proton conductivity refers to the ability of materials to transport protons and is a central property in a variety of applications such as fuel cells,[29] electrochemical sensors,[30,31] and proton exchange membranes.[32] The development of solid-state proton conductors is an important emerging field, especially for fuel cells. In this area of research, several groups have constructed these materials employing DCC methodologies.[33] Dichtel, Rolandi and co-workers,[34] used DCC to synthesize diverse proton-conducting supramolecular nanotubes (**Figure 2**). Their strategy involves the synthesis of macrocycles of different shapes, channel sizes and chemical functionalities using a ditopic amine building block decorated with a pyridine ring. The condensation of this 2,4,6-triphenylpyridine-based diamine with various aromatic ditopic aldehydes results in the formation of chemically distinct pentagonal, hexagonal, and diamond-shaped macrocycles depending on the dialdehyde monomer's substitution pattern and geometry (**Figure 2**). DCC here allows for a fast synthesis of diverse functional macrocyclic derivatives from relatively simple precursors. Protonation of these macrocycles under mild conditions leads to their assembly into nanotubes. These nanotubes exhibit proton conductivities up to 10^{-3} S m^{-1}, and their internal pore sizes influence their conductivity values.

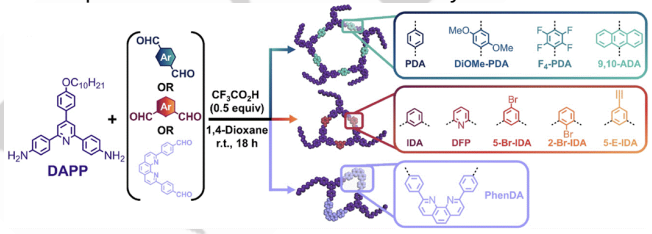

Figure 2. Modular synthesis of imine-linked macrocycles from a pyridine-containing diamine monomer.[34] Reprinted with permission from ref. [34]. Copyright 2021 American Chemical Society.

DCC proved to be helpful to prepare porous organic cage.[35] In 2016, Cooper, Hardwick and co-workers prepared cage **1a** and **1b** via imine condensation. This cage was further engaged in a reduction step affording amine-linked cage **2a** before being protonated to yield cage **3a** bearing ammonium moieties (**Figure 3**).[36] Reductive aminations are commonly used to lock imine-based structures into kinetically inert amine-bound materials. The protonated versions of these molecular cages show proton conductivities up to 10^{-3} S cm^{-1}. These values are similar to proton-conductive metal-organic frameworks.[37] The nanoconfinement of water molecules into the cavity of the organic cage together with its flexibility, which gives access to hydrogen bond reorganization, boost proton transfers. In addition, the multi-dimensional nature of the organic cage's conduction pathway leads to improved proton conductivity.

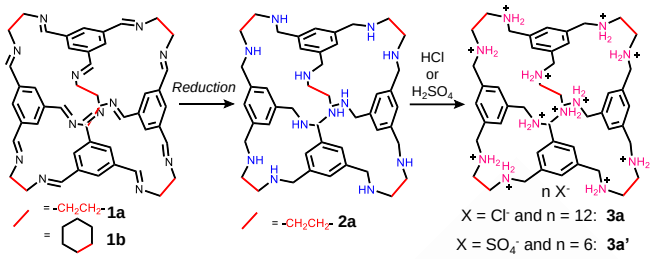

Figure 3. Structures of molecular proton conductors based on imine organic cage **1a/b**, amine **2a** and salt forms **3a/b**.[36]

In 2018, Wu and Han[38] have described the enhancement of the proton conductivity of recast Nafion employing a composite material prepared from Nafion and cage **1b**. This improvement of the proton conductivity in the composite proton-exchange membrane is originated from its crystalized porous organic cage **1b**. Two years later, Di, Zhuang, and co-workers[39] further improved the proton conductivity of proton exchange membranes incorporating dynamic porous organic cage **1b**, reaching a value of 0.315 S cm^{-1}, employing sulfonated polyethersulfone nanofibers. The study demonstrates that nanofibers containing porous imine cages can form long-range proton conducting channels, leading to improved performances of the proton conductivity. In these examples, DCC is exploited to assemble simple compounds into functional materials, but the dynamic character of imines does not seem to be a desired featured of the final architecture.

3.1.2 Organic Light-Emitting Diodes (OLEDs)

In 2019, Yang and co-workers[40] described how DCC is used to synthesize organic cage **4** in almost quantitative yield (**Figure 4**). The dynamic nature of the imine bonds enables the extremely efficient formation of fluorescent cage **4** featuring two tetraphenylethylene (TPE) units, which are commonly employed as aggregation-induced emission (AIE) luminogens,[41] under thermodynamic control. The rigid stacked structure of the cage lead to the suppression of intramolecular rotations and vibrations of the phenyl rings allowing a strong fluorescence in both the solid state (Φ_{PL} = 83%) and dilute solutions (Φ_{PL} = 82% in DMSO), whereas the monomeric unit follows an AIE behavior. Cage **4**

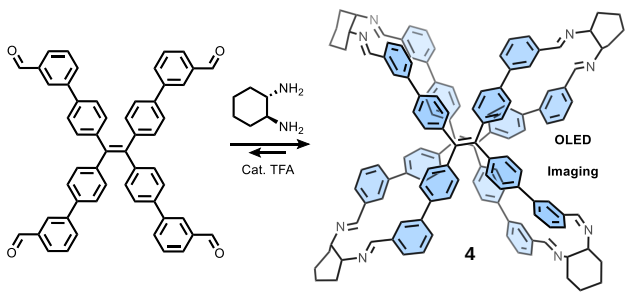

Figure 4. Synthesis of TPE-based organic imine stack using DCC.[40]

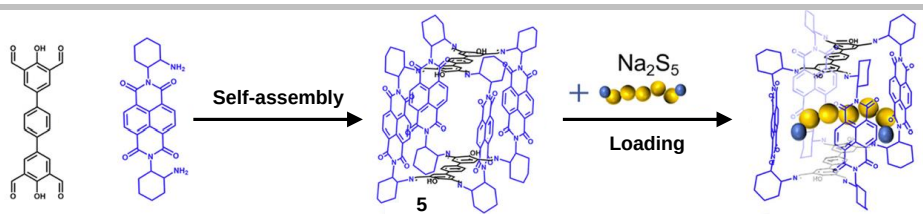

Figure 5. Self-assembly of organic cage **5** and the encapsulation of Na_2S_5.[44] Adapted with permission from ref. [44]. Copyright 2019 American Chemical Society.

exhibits high thermal and chemical stabilities, as well as excellent solubility in common solvents. **4** has been used as emitter in solution-processed electroluminescent devices with high brightness and external quantum efficiency. Additionally, cage **4** has been utilized as fluorescent probe for lysosome imaging. DCC allows this property to emerge by carefully arranging the chromophore in space in a way that promotes fluorescence.

Imines have been also used to assemble other chromophores of interest. Two conjugated near-infrared acceptor-donor-acceptor isatin Schiff bases were employed as emissive layer in OLEDs.[42] The electroluminescent spectra of these materials range from 630 to 700 nm, with band gaps measured between 1.97 and 1.77 eV. It is must be noted that the authors do not comment on the stability of the final materials in these two examples.

3.1.3 Organic Batteries

An additional feature of DCC is its ability to produce soluble materials suitable for applications in batteries as organic conductors. An illustration of this is the work conducted by Chen, Shen, Cooper, Qiu and co-workers[43] where protonated organic cage **3a** (**Figure 3**), was loaded with lithium cations by addition of $LiClO_4$. The resulting material was then utilized as a conductor in all-solid-state lithium batteries. These Li^+ conducting porous organic cages can be dissolved in a cathode slurry and recrystallize onto the surface of the cathode particles during the coating process, forming an effective ion-conducting network. The organic cage-based solid-state Li^+ conductor exhibits high ionic conductivity at room temperature, high solubility in polar solvents, wide electrochemical window, and high ion transference. The catholyte has shown compatibility with several cathode active materials, including $LiFePO_4$, $LiCoO_2$, and $LiNi_{0.5}$-$Co_{0.2}Mn_{0.3}O_2$, leading to all-solid-state lithium batteries that exhibit satisfactory electrochemical performance at room temperature. Here again the imine is efficiently used to self-assemble the cage but its dynamic nature is not exploited.

Song, Zhang and co-workers[44] have employed organic cage **5** bearing four NDI units in order to bind polysulfide species, and they have used it as a lithium-sulfur anode in lithium-ion sulfide batteries (**Figure 5**). The authors developed this organic cage to address the limitations of conventional lithium-ion batteries in applications requiring higher power and energy, such as electric vehicles and grid-scale applications. The organic cage has a good adsorption capacity for sodium polysulfide, which seems crucial for stabilizing the battery's performance. The authors conducted experiments and tests to evaluate the performance of the organic cage **5** as a sulfur-anchoring material in lithium-sulfur batteries. They found that the cage exhibited a high specific capacity and good stability with minimal capacity fading after multiple charge-discharge cycles.

Recently, Gordon, Smythe and co-workers[45] have reported the use of iron-based iminopyridine complexes as charge carriers for non-aqueous redox flow battery applications. The self-assembled complexes exhibit multiple reversible redox events over a wide voltage range. This redox behaviour makes them capable of accepting and donating multiple electrons enabling efficient energy storage and discharge. The authors emphasize the importance of developing charge carriers with properties such as multiple reversible electron transfers, stability in oxidized and reduced forms, high solubility, and low cost. The use of high denticity ligand systems, earth abundant metal centers, and cheap precursors assembled by DCC shows potential for constructing high energy density materials for grid-scale energy storage applications. Again, in these examples, DCC is a convenient way to assemble materials in a one pot reaction on account of DCBs, nevertheless, the dynamic nature of DCBs and its influence on the device performances are not explored.

3.1.4 Charge Separation and Photocatalysis in Self-Assemble cages

Organic molecular cages prepared by DCC, especially those featuring imine bonds, represent a simple way to self-assemble chromophores into well-defined photoactive structures. In 2019, Ke, Zhang and co-workers have reported chiral cage **6** featuring four perylene diimides (PDIs) and two TPE units (**Figure 6a**).[46] Cage **6** exhibits photoinduced intramolecular charge-separation properties which can be tuned by the addition of polycyclic aromatic hydrocarbons since the latter bind strongly to the cage, entering in its cavity. This electron-deficient cage can be efficiently used as visible-light photocatalyst for Smiles rearrangements.

Šolomek, Coskun and co-workers, later, synthesized chiral rylene diimide cages of various porosity by varying the size of the rylene diimide employed during imine bond formation (**Figure 6b**).[47] These porous electron-deficient cages exhibit good gas adsorption properties and selectivity. Interestingly, the PDI-based cage **7** shows delayed fluorescence, due to an intramolecular charge separation event upon light-irradiation. In these two examples, DCC is used to self-assemble small compounds into complex architectures from which new properties emerge, but the dynamicity of the materials is not further explored. The structures here illustrate a promising strategy to produce complex multichromophoric architectures for application in confined photocatalysis and beyond.[48,49]

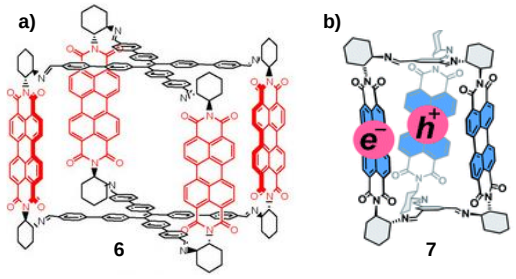

Figure 6. Self-assembled PDI cages from a) Ke and Zhang,[46] and b) Coskun and Šolomek.[47] Adapted with permission from ref.[46] Copyright 2019 Wiley-VCH. Adapted with permission from ref. [47] Copyright 2014 Wiley and Royal Society of Chemistry.

10.1002/ejoc.202400211

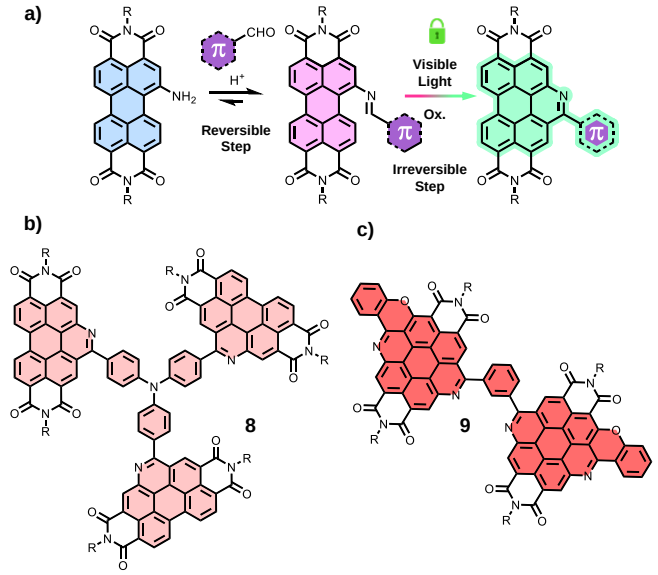

Figure 7. a) Light-locked dynamic covalent synthesis of AzaBenzannulated PDIs.[50]. NFAs employed for OSCs based on b) azabenzannulated PDIs trimer **8** and c) *ortho* O-annulated BACD dimer **9**.

3.1.5 Organic Solar Cells (OSCs)

In the past few decades, the development of organic solar cells (OSCs) has been considerably growing.[51,52] Nevertheless, the use of DCC reactions to construct small organic compounds for this application remains limited on account of the poor conjugation of a wide number of DCBs. In our group, we focused our attention on a one-pot light-mediated azabenzannulation reaction[50,53] between aldehydes and PDIs bearing amine moieties in the *bay* positions. This reaction proceeds via the formation of an imine bond which is, then, photocyclized and finally oxidized to afford the desired heterocycle. In this case, the first step is a DCC reaction, while the second and the third steps lock the DCB (**Figure 7a**). Furthermore, the generation of this heterocycle allows the electronic conjugation between both components of the molecule. In this context, we have designed a series of azabenzannulated PDIs bearing different heteroatoms, *i.e.* N, S, Se, on the other *bay* position of the PDI. These n-type semiconductors were found to have moderate electron mobilities in the range of 10^{-3} cm^2 V^{-1} s^{-1}.[54] Encouraged by these results, we have synthesized azabenzannulated PDI multimers (**Figure 7b**) employing the same methodology. These extended PDIs were utilized as non-fullerene electron acceptors (NFAs) for bulk-heterojunction OSCs. The power conversion efficiency (PCE) of these organic photovoltaic devices reached 1.9% on blends of azabenzannulated PDI multimers **8** with the PM6 polymer.[55] In addition, employing two consecutive light-driven azabenzannulation reactions followed by a post-functionalization reaction on regiopure 1,6-diamino-PDI,[56] we were able to synthesize a bis-azacoronene diimide (BACD) dimer **9** doped with oxygen atoms (**Figure 7c**). The electron-poor compound **9** was exploited as a NFA in bulk-heterojunction OSCs. Blends of this compound with PTB7-Th donor polymer afforded an average PCE of 1.43%.[57] We strongly believe that this chemical transformation involving a DCC reaction which is subsequently locked is of major interest for the development of organic semiconducting materials.

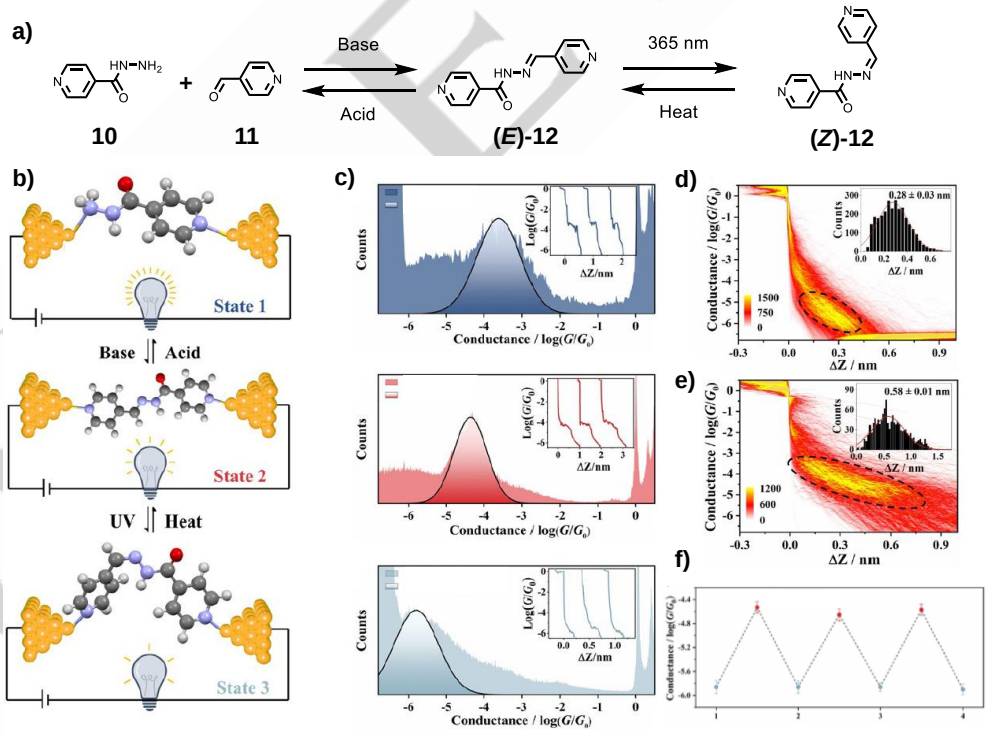

Figure 8. (a) Formation of compound **(*E*)-12** bearing a dynamic covalent bond which can be isomerized under light and heat. (b) cartoon representation of the three possible states of this single-molecule junction in solution depending on the applied stimuli. State 1 corresponds to the molecular junction of compound **8** State 2 corresponds to the molecular junction of compound **(*E*)-12** and State 2 corresponds to the molecular junction of compound **(*Z*)-12**. (c) 1D conductance histograms constructed from compound **(*E*)-12** in the presence of CF_3CO_2H (up), in the absence of acid (middle) and following irradiation at 365 nm (down). 2D histograms of conductance versus relative distance (Δz) of (d) **(*E*)-12** and (e) a solution of **(*E*)-12** after irradiation with a 365 nm UV lamp. (f) Conductance values obtained for a solution of **(*E*)-12** after successive irradiation with a 365 nm UV lamp (red dots) and heating at 65°C (blue dots). This photo-thermal stimulation of the dynamic hydrazone bond in **12** is reversible at least for four cycles.[61] Reprinted with permission from ref. [61]. Copyright 2021 Wiley-VCH.

3.2 Hydrazone Exchange

The hydrazone exchange[58–60] is a dynamic covalent chemistry reaction between aldehyde and hydrazine moieties, sharing several similarities with the aforementioned imine exchange. In basic medium, the dynamic covalent bond, *i.e.* the hydrazone group, is formed by reaction between the two precursors and is stable, while in acidic medium this bond remains labile. In 2021, Hong and co-workers employed compound **12** in single-molecule junctions.[61] Compound **(*E*)-12** is formed by reaction of acyl hydrazine **10** and aldehyde **11** under basic conditions and possess a hydrazone dynamic covalent bond, which can be isomerized upon exposure to light and heat (**Figure 8a**). These reactions allow three states in molecular junctions depending on the stimulus applied in solution (**Figure 8b**). The observation of these three states was performed by scanning tunneling microscopy break-junction. The conductance obtained are substantially different and well-defined depending on the applied stimuli, therefore, on the three states (**Figure 8c**). The authors went further by reversibly switching between these states. By successive addition of CF_3CO_2H and Et_3N in a solution of (***E*)-10**, the hydrazone dynamic covalent bond was cleaved and locked resulting in a change in the conductance at the single-molecule junctions. Similarly, by successive irradiation with a 365 nm UV lamp and heating at 65°C, the hydrazone dynamic covalent bond was isomerized from its **(*E*)-12** (**Figure 8d**) to its **(*Z*)-12** configuration (**Figure 8e**) affording two different conductance values as it can be seen on the 2D conductance histogram of both states. It is worth highlighting that both of these switches were performed for four complete cycles showing the reversibility of the system (**Figure 8f**). This observation demonstrates the importance of the dynamic covalent chemistry in the design of switchable organic electronic devices and sensors since the dynamic hydrazone bond could potentially afford stimuli responsive devices.

Recently, Wei and co-workers[62] have built a field-effect transistor (FET) sensor of Cu^{2+} by employing a graphene-based FET doped with pyrene-1-carboxaldehyde hydrazone possessing a limit of detection of 5.0×10^{-20} mol L^{-1}. In the presence of H_2O and Cu^{2+} the dynamic hydrazone covalent bond of pyrene-1-carboxaldehyde hydrazone was cleaved and an aldehyde was formed. This change on the FET surface can be detected on account of the distinct doping effect of the pyrene molecules with aldehyde or hydrazone moieties which changes the performances of the FET. In these two selected examples, both the ease of preparation and the dynamic, reversible character of the hydrazine are being used to build stimuli-responsive functional electronic devices.

3.3 Dichalcogenide Dynamic Covalent Bond

The dynamic covalent chemistry of disulfide bonds[63–66] is well-known, naturally occurring in proteins,[67,68] gave rise to a great number of supramolecular architectures,[69,70] and has found multiple applications in sensing and chemical biology.[71] Sulfur, on the other hand, has been extensively employed, together with lithium, to afford lithium–sulfur batteries.[72–74] Organosulfur molecules or materials[75] have, therefore, been used for the construction of rechargeable lithium batteries. Some of these batteries exploit molecules with dynamic disulfide bonds in various manner, such as cathode materials[76–78] or electrolyte[79] for lithium batteries, as well as additive[80] for alkaline

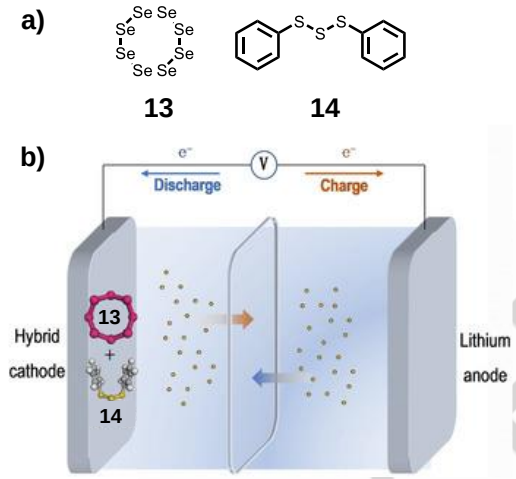

Figure 9. (a) Compounds used for the construction of Fu's organic-inorganic hybrid cathode and (b) a cartoon representation of the battery possessing a lithium anode and the hybrid cathode.[83] Reprinted with permission from ref. [83]. Copyright 2019 Wiley-VCH.

aluminum/air batteries, to improve their performances. Other chalcogen elements, such as selenium[81] and tellurium,[82] have also the ability to form such dynamic covalent bonds. Thus, Guo and Fu reported the use of Se−Se dynamic covalent bond in Li−Se batteries by employing diphenyl diselenide as additive electrolyte.[84] This additive improves the robustness and cycling stability of the Li−Se batteries. Furthermore, a better electrochemical performance in rechargeable lithium batteries was discovered when using electrolytes or additives with molecules possessing a DCB with two distinct chalcogen elements, such as S−Se[85] or S−Te,[86,87] compared to similar molecules with two identical chalcogen elements. In 2021, Fu and co-workers have built (**Figure 9**) an organic-inorganic hybrid cathode with Se_8 (**13**) and diphenyl trisulfide **14** in order to benefit from the efficiency of the reduction of lithium polysulfide and the high conductivity of the selenium.[83] During the charge-discharge processes occurring in the battery, various species containing S−S, S−Se and Se−Se bonds are formed on account of the dynamic covalent dichalcogenide chemistry, enhancing the stability of the cathode. The performances of the cell constructed with this hybrid cathode are outstanding reaching a capacity of 96.5 % compared to the theoretical specific capacity for the first discharge. Furthermore, a remarkable Coulombic efficiency, beyond 99 %, is measured for this organic-inorganic hybrid cathode after 250 cycles. In these examples, chalcogen-chalcogen exchange reactions are seemingly taking place in the devices and the authors often state that this dynamicity is the reason of the high performance that they observe. Thus, the DCC of dichalcogenide exchange reactions have a promising future for building batteries, even if, at this stage, the mechanism behind the improvement of performances due to DCC is not perfectly understood and remains to decipher.

3.4 Other Dynamic Covalent Bonds

In 2016, Moore and co-workers[88] reported the synthesis of kinetically trapped porous organic cage **15** employing the dynamic covalent chemistry behavior of the alkyne metathesis reaction.[89] In the presence of an appropriate metal-catalyst, alkyne metathesis becomes reversible and thus such systems behave as

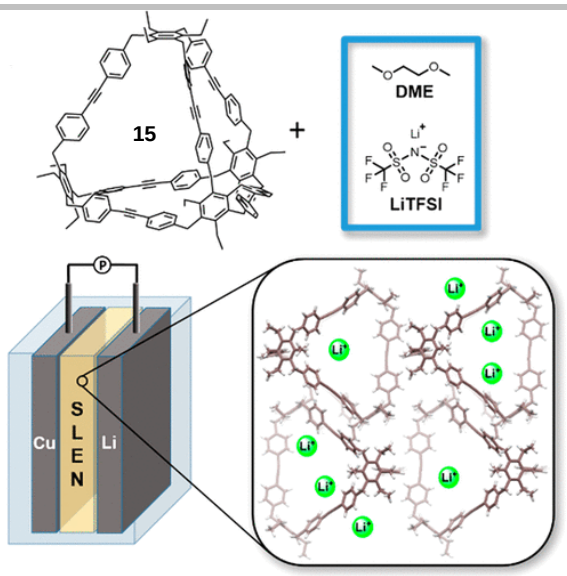

Figure 10. Kinetically trapped porous organic cage **15** synthesized via alkyne metathesis and employed in solid–liquid electrolyte nanocomposites (SLEN) with LiTFSI and 1,2-dimethoxyethane (DME).[90] Reprinted with permission from ref. [90]. Copyright 2018 American Chemical Society.

DCBs which are then kinetically trapped once separated from the catalyst. Two years later, Moore, Nuzzo and Gewirth described the use of porous organic cage **15** (**Figure 10**) in a solid–liquid electrolyte nanocomposites (SLEN) system composed of cage **15**, bis(trifluoromethane)sulfonamide lithium salt (LiTFSI) and 1,2-dimethoxyethane (DME).[90] The SLEN material obtained from the molecular cage **15** is a superionic conductor since it displays a remarkable ionic conductivity ($\sigma = 1 \times 10^{-3}$ S cm^{-1}) at room temperature with a low activation energy of 0.16 eV.

The Se−N DCB[81,91] have been utilized by Feng and Feng to reversibly tune the electron and hole mobilities of a nitrogen-doped graphene-based FET (**Figure 11**).[92] In the presence of phenylselenyl bromine the surface of the nitrogen-doped graphene is modified since Se−N dynamic covalent bonds are formed. These Se−N dynamic covalent bonds can be cleaved by heating between 60 and 130 °C. The FET based on the nitrogen-doped graphene exhibits a n-type conduction while the modification of the surface by the introduction of the Se−N dynamic covalent bonds renders the conduction of the FET to be a p-type. By increasing gradually the temperature from 30 to 130 °C, the Se−N dynamic covalent bonds are progressively cleaved leading to a change of the conduction of the FET from p- to n-type, together with an increase in the electron and hole mobilities. Remarkably, this process is reversible on account of the dynamic covalent chemistry behavior of the Se−N bond.

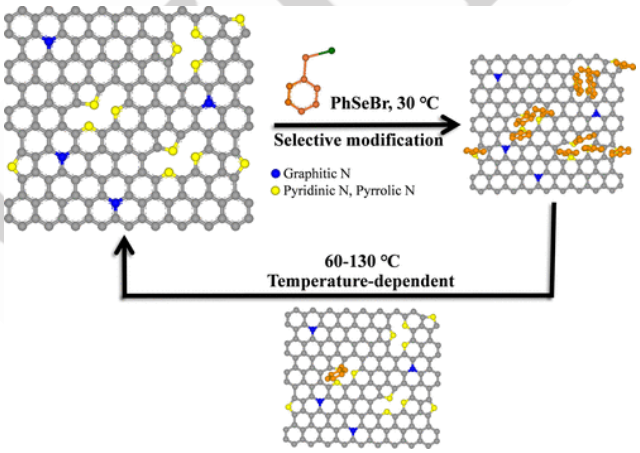

Figure 11. Illustration of Feng and Feng's nitrogen-doped graphene modified by the addition of phenylselenyl bromine and exhibiting temperature-dependent Se−N dynamic covalent bonds. [92] Reprinted with permission from ref. [92]. Copyright 2019 American Chemical Society

As an outlook, we wish to mention the Michael addition, which is another reversible reaction that has been exploited for the construction of hydrogels,[93] self-healing polymers,[94] and recyclable materials.[95] The Michael addition reaction has found a myriad of bio-applications,[96] especially with fluorescent probes as Michael acceptors.[97] Indeed, the Michael addition to these probes can affect their luminescence properties leading to the design of numerous stimuli-responsive live cell imaging probes and sensors.[98] We believe that the use of this dynamic covalent reaction can open up many opportunities for the design of stimuli responsive emissive organic electronic materials.

4. Dynamic Covalent Conjugated Polymeric Materials

4.1 Polyimines and Polyazines

4.1.1 Polymers Prepared by Direct DCC Reactions

A wide range of stimuli-responsive dynamic covalent polymers have been prepared by taking advantages of various DCBs, in order to developed self-healing or smart materials.[99,100] Dynamic covalent polymers are much less represented in optoelectronic applications, even though the perspective to prepare conjugated polymers for organic electronics and biomedical applications[101] by DCC is a very attracting alternative to metal-catalyzed reactions. In this category of material, imines and azines are immensely dominating. Dynamic polyimines can be used to give polymers a dynamic and/or sensitive optoelectronic properties. Matile and co-workers have developed amphiphilic conjugated polyimines that could be used as multifunctional optical sensors of the organization of lipid bilayer membranes.[102] In liquid

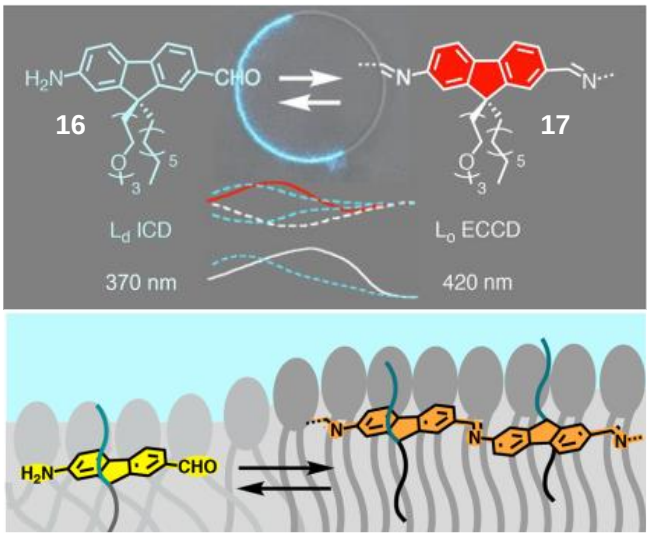

Figure 12. Membrane-organization-sensitive dynamic covalent polymerization affording a fluorescence readout on membrane ordering.[102] Reprinted with permission from ref. [102]. Copyright 2018 American Chemical Society

10.1002/ejoc.202400211

disordered (L_d) membranes, the amino formyl fluorene unit **16** does not polymerize and thus monomer **16** remains fluorescent, while in liquid ordered (L_o) phases, a polymerization happens leading to non-emissive polymers **17** (**Figure 12**). This dynamic system built from a simple molecule renders possible the visualization of membrane phases by confocal microscopy in model vesicles. This example shows how dynamic polymerization can be used to detect a change in the environment when combined with an optical readout. Another interesting example of opto-electroactive self-assembled polymer was reported by Nitschke and co-workers. They prepared extended supramolecular metallohelicates incorporating copper atoms.[103] By adjusting the geometry and stoichiometry of the components of the polymer and the reaction conditions, the length of the organometallic wires can be controlled.[104] Under an electric field, the copper atoms in these wires oxidize from Cu^{I} to Cu^{II}, turning the assembly into a mixed-valence structure.[105] This change in the copper atoms oxidation state leads to a 10^4 fold increase of conductivity compared to the polymer incorporating only Cu^{I} atoms. Moreover, another version of these organometallic structures built from a phenanthroline ligand has been used as the active material of an electroluminescent device emitting white-blue light.[106] These examples show that DCC can be used to self-assemble macromolecular architectures into functional stimuli-responsive architectures from simple components.

A stimulating perspective for the future of organic electronics is to prepare organic conjugated polymers by taking advantage of efficient DCBs-based polymerization instead of precious-metal catalyzed reactions and to introduce stimuli-responsive properties in these materials (**Figure 13a**). We have selected a few examples illustrating the fabrication of materials used in electronic devices such as organic field-effect transistors (OFETs) and OSCs. First, azine linkages[107] can be efficiently prepared by combining hydrazine with ditopic aldehydes (**Figure 13b**). Li and co-workers reported a high-performance ambipolar semiconductor based on π-conjugated polyazine containing diketopyrrolopyrrole units.[108] The polymerization has been conducted in two steps by refluxing the monomer with hydrazine

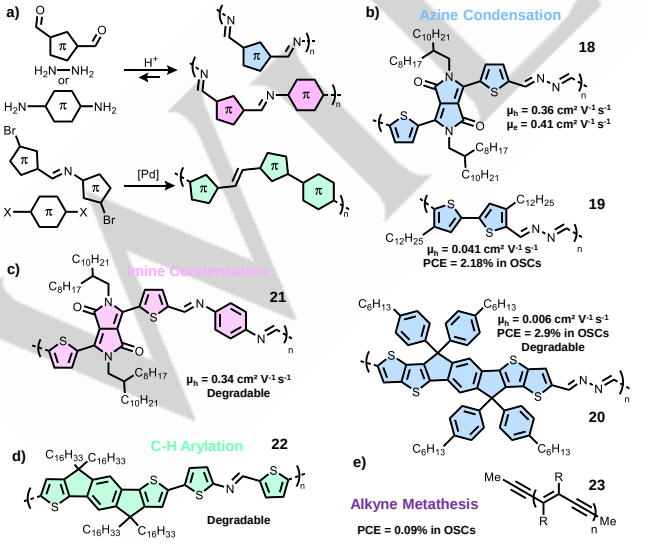

Figure 13. a) Synthetic strategies used to synthesize azine/imine-incorporating conjugated polymers for semiconducting applications. Examples of polymers prepared by b) azine condensation, c) imine condensation and d) Pd-catalyzed direct C-H arylation. e) Example of a conjugated polymer obtained by dynamic covalent alkyne-metathesis polymerization.

monohydrate in a mixture of $CHCl_3$ and ethanol and by refluxing the oligomer in 1,1,2-trichloroethane. A maximum molar mass of 102 kg mol^{-1} has been reached with a polydispersity index of 4.3. After purification through Soxhlet extractions, the final polymer **18** have been evaluated as an active layer in an OFET device exhibiting a very good electron mobility of up to 0.41 cm^2 V^{-1} s^{-1} and a hole mobility of up to 0.36 cm^2 V^{-1} s^{-1}. The final polymer displayed good stability under gate stress and did not show any decomposition below 300 °C. Another example from the same group reports the successful synthesis of a bithiophene-azine polymer that was incorporated in OSCs as a donor material.[109]In this case, the polymerization was conducted by refluxing the monomer with hydrazine acetate in $CHCl_3$. The polymer **19** was end-capped before terminating the polymerization and reached a maximum molar mass of 21.8 kg mol^{-1} with a polydispersity index of 1.58. **19** showed good stability once incorporated into OSCs, with only 10% drop in PCE after 200 h of storage under ambient conditions. It demonstrated the robustness of the dynamic linkage in these conditions. The device reached modest, yet promising, PCE up to 2.18%. In addition, this polymer exhibited hole mobilities of up to 0.041 cm² V^{-1} s^{-1}. The group of Kuwabara also tackled the synthesis of conjugated polymers containing azine bonds in their main chains.[110] One of the polymers, an end-capped di-*n*-octylfluorene-dicarboxaldehyde-based material, displayed a maximum molar mass of 20.6 kg mol^{-1} with a polydispersity index of 2.1. The same synthetic strategy has been also applied to the preparation of a polymer based on a more complex dialdehyde IDTTB6 monomer, a strong donating group commonly employed in the design of high-performance materials for OSCs.[111] Polymer **20** has been evaluated as a p-type semiconducting material in OFETs, showing moderate hole mobilities of 0.006 cm² V^{-1} s^{-1}. OFETs stored in the dark and in open air for 4 days exhibited similar hole mobilities indicating a decent resistance to hydrolysis and oxidation. In addition, the azine-based polymer **20** was classified again as a p-type material and tested in bulk-heterojunction-type OSCs showing a PCE of 2.9%. To test the stability of the DCBs, azine-based polymer **20** was dissolved in wet chloroform for several hours and did not show any degradation according to size-exclusion chromatography measurements. However, this polymer showed a slight decrease in molar masses after contact with a diluted aqueous acetic acid solution for 24 h at room temperature, probably due to a progressive hydrolysis of the sensitive linkage. The syntheses of polyazines illustrated here presents a dynamic character and are efficient synthetic tools to prepare conjugated polymers circumventing the use of precious-metal catalyst and organotin derivatives.

The imine bond has also been employed to prepare conjugated 1D macromolecules (**Figure 13c**) but this time often with the aim of constructing degradable organic semiconductors for the development of non-invasive, recyclable or bio-compatible electronics,[112] since such systems have great potential as sensors for in-situ monitoring. Bao and co-workers have reported the use of semiconducting polymers based on reversible imine bonds for their implementation in thin-film transistors.[113,114] These diketopyrrolopyrole-based polymers were synthesized by imine condensation reaction with *p*-phenylenediamine under acidic conditions. These polymers attained a high molar mass of 39.6 kg mol^{-1}. Polymer **21** showed good stability under ambient conditions but was totally disintegrated under acidic conditions after 40 days in solution or in thin films. This polymer was spin-

coated onto an ultrathin cellulose substrate in order to prepare a thin-film OFET-based biosensor. The bottom-gate/top-contact device showed a very good hole mobility of up to 0.34 $cm^2 V^{-1} s^{-1}$. Moreover, the flexible devices were totally disintegrable after 30 days in a pH 4.6 buffer solution mixed with cellulase. More recently, Tran and co-workers described the use of imine polycondensation to obtain bio-based degradable conjugated polymers employing carotenoids and *p*-phenylenediamine-based monomers.[115] Degradation studies were conducted in hydrochloric acid and revealed a complete depolymerization, yielding starting monomers, on account of the imine cleavage under acidic conditions. The influence of artificial sunlight on the rate of acid hydrolysis was demonstrated concomitantly with a higher loss in absorbance when the polymer was exposed to light. Such imine-bonded conjugated polymers prepared from bio-available starting materials are potential sustainable semiconductors, nonetheless, their semiconducting properties have not been evaluated in this study.

4.1.2 Polymers Prepared by Pd-Catalyzed Cross-Coupling Reactions

Another strategy has been proposed to introduce dynamic linkages into semiconducting polymers. Azine and imine moieties can be indirectly introduced as cleavable linkages into semiconducting polymers by polymerizing azine- or imine-containing monomers through palladium-catalyzed cross-coupling reactions (**Figure 13a/d**). This strategy allows chemists to avoid the competing hydrolysis happening concomitantly with the elongation of the polymer chain when using DCB-based polymerization reactions. Li and co-workers utilized this method to create azine-based donor-acceptor conjugated polymers.[116] These polymers were obtained by Stille coupling polymerization in a high molar mass of 49.8 kg mol^{-1} and a good polydispersity index of 1.76. The resulting materials were tested as semiconductors in thin film transistor devices showing relatively balanced ambipolar charge transport characteristics with a good hole mobility of up to 0.11 $cm^2 V^{-1} s^{-1}$ and an electron mobility of up to 0.035 $cm^2 V^{-1} s^{-1}$. In this case, the stability of the DCB has not been investigated, the azine linker has been employed to lower the LUMO energy level of the material. Tran and co-workers exploited a similar strategy to introduce imines into conjugated polymers by Pd-catalyzed C−H direct arylation.[117] The imine motif provided a stimuli responsive character to the polymer **22** by changing its optical properties depending on the protonation state of the nitrogen atom of the imine. At very low pH, the imines were progressively hydrolyzed. This study paves the way for the synthesis of degradable conjugated polymers prepared by Pd-catalyzed reactions. Overall, the introduction of DCBs in conjugated polymers have been successfully exploited both as a synthetic tool and a way to introduce a new function. However, materials prepared *via* these strategies remain overall modest in term of performances compared to state-of-the-art materials in the field, even if some of them display high and useful charge mobilities.

4.2 Polydiacetylenes

Qin and co-workers employed the alkyne metathesis reaction to synthesize novel polydiacetylenes using acyclic enediyne metathesis polymerization of methyl terminated *trans*-enediyne monomers (**Figure 13e**).[118] By using a highly active alkyne metathesis catalyst, the polymers attained a maximum molar mass of 15.6 kg mol^{-1} with a polydispersity index of 1.9. The final soluble polymers **23** were used as donors, blended with phenyl-C_{61}-butyric acid methyl ester (PCBM) as acceptor in bulk heterojunction OSCs exhibiting a modest PCE of 0.09%. Unlike the aforementioned azine/imine-linked polymers, the particularity of this synthetic strategy is that it relies on a dynamic covalent reaction while the final material is kinetically inert.

5. Covalent Organic Frameworks (COFs)

COFs are crystalline 2D or 3D organic networks of well-defined structural parameters and pore size. They are synthesized through the condensation of two or more components with well-orientated reacting groups to allow the progressive growth of a repeating motif.[119] It can be difficult to obtain defect-free and crystalline materials with reactions affording strong and kinetically inert covalent bonds. Indeed, the irreversible formation of defects or undesired poorly organized growth of the material can prevent the formation of a well-defined crystalline network. Yaghi and co-workers first described how to use DCC to overcome this issue.[120,121] The dynamic character of imines or boronate esters, the most common examples, allows the network to self-correct and grow following the more thermodynamically stable motif, driven by the orientation of the functional groups existing on the building blocks. Functional groups required to perform DCC can be installed on various redox and optically active molecules affording a wide variety of COFs architectures, compositions and properties. These materials have found applications in energy/gas storage, separation, sensors, heterogeneous (photo)catalysis for example for the photosynthesis of H_2 and more.[122–127] To keep the discussion centered on the relationship between DCBs and COFs functionalities and properties, we will focus on the specific cases of imine-base COFs, the most represented class of material implemented in organic electronic devices, and dynamic S_NAr-based COFs, a more recently developed approach.

5.1 Imine-Based COFs

Imine-based COFs (**Figure 14a**) are promising materials for organic electronics since they offer the potential to create fully conjugated networks. For this reason, imine-based COFs have demonstrated strong potential in various applications, such as organic photovoltaics,[128,129] charge transport,[130,131] and photodetectors.[132] We will not focus our attention, in this review, on the performances of such materials, since they have been extensively surveyed in previous reports.[123,125,133] We will, however, briefly discuss the use of DCBs to understand how they shape the design and stability of COFs. The dynamicity of imines is crucial for the formation of a repeating crystalline motif. This property, however, remains in the final material and originates several central issues to the design of COFs, as stated by prominent researchers in the field during the past few years.[134] Imine-based COFs are facing a trilemma: they should combine stability, crystallinity, and efficient conjugation. Regarding the stability of these materials, the imines remain dynamic, and therefore are sensitive to moisture, acids, bases, and strong nucleophiles. This limitation restricts the use of these materials in applications where they could be exposed to harsh conditions or chemical stress. Imine-based COFs are also less thermally stable compared to other COFs, especially those bearing boronate ester units.[135] Furthermore, imine linkages are relatively flexible, and

therefore, reduce the overall crystallinity of the network and the efficiency of the conjugation between electroactive units. Thus, the electronic communication through the imine bond is of lesser efficiency compared to that through alkenes,[136,137] which directly limits the performances of these materials. To avoid this issue, several strategies, such as tautomerism stabilization of the imine bond[138] or post-synthetic cyclization reactions[139,140] of the imine have emerged (**Figure 14a**) and have different outcomes.[141] Regarding the post-synthetic cyclization method, the final functional groups obtained by such transformations can directly have a strong impact on the final optoelectronic properties of the COF. In addition, oxidation[143] or reduction[144] of the imine bonds into amide or amine moieties will considerably diminish the electronic communication in the final COFs. It must be highlighted that a large set of strategies to stabilize imines *via* a post-functionalization approach have been reported and were summarized elsewhere.[145,146] Although encouraging results and significant improvement have been observed on the crystallinity

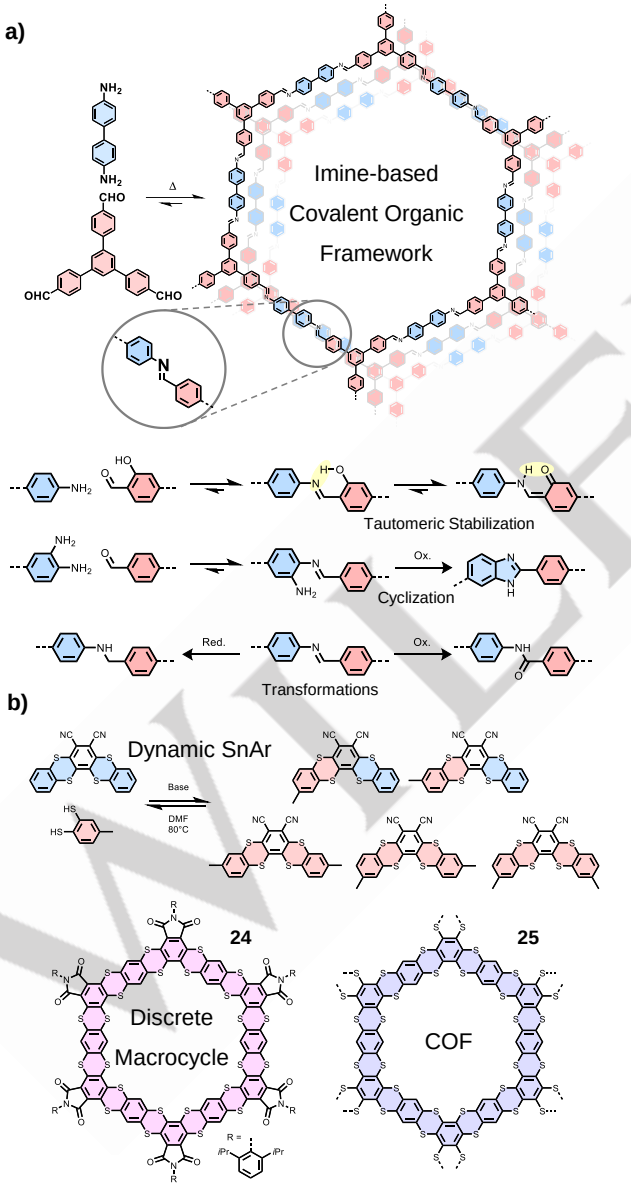

Figure 14. a) Example of an archetypal Covalent Organic Framework (COF) and selected illustrations of strategies for the post-synthetic stabilization of the imine bond. b) Dynamic SnAr illustrated by a scrambling experiments (top) and examples of macrocycles and COFs obtained *via* this method (bottom).[142]

and stability, these transformations do not always go together with an improvement of electronic performances. Liu, Inkpen and co-workers investigated the conductance through dynamic covalent bonds, *i.e.* imine, boronate ester, diazaborole, and functional groups resulting from post-functional transformations, *i.e.* imidazole, by installing single model molecules between gold electrodes employing a scanning tunneling microscope-based break-junction method.[147] The measured conductance were modest, nonetheless they demonstrated that the imine units is the most conductive of these motifs. All together, these observations demonstrate that it is still crucial to develop easy to apply, non-invasive, functional-group-tolerant post-synthetic imine-transformation strategies to turn COFs into lasting materials.[145] However, in order to push the boundaries of their optoelectronic performances, these transformations should afford new functional groups or bonds that will improve (or at the very least not damage) the electronic conjugation as well as the charge mobility at the nanoscopic scale, and thus the conductance at the macroscopic scale. Moreover, other fields could benefit from the different post-synthetic lock strategies on DCBs developed in the context of COFs to obtain non-dynamic discrete objects which would be easier to isolate and investigate. An exotic case, that stands out, is the synthesis of graphyne: a COF prepared by dynamic covalent alkyne metathesis.[148] As in the previously cited compounds or materials featuring the alkyne metathesis reaction, the final material is kinetically locked in absence of the catalyst.

5.2 Dynamic S_NAr

Dynamic Nucleophilic Aromatic Substitutions are becoming increasingly attracting tools for the synthesis of conjugated networks. A seminal work from Swagger and co-workers demonstrated that dynamic self-correcting nucleophilic aromatic substitution between polytopic aromatic thiols and fluorinated aromatic molecules of specific orientation could efficiently lead to sulfur-rich discrete molecules, macrocycles **24** and 2D crystalline networks **25** in controlled stoichiometry (**Figure 14b**).[142] The yields of these reactions are excellent and these reactions are highly selective. The resulting thianthrene-based electroactive p-type ladder materials are promising for applications in energy storage applications. A few years later, the group of Kaskel exploited this reaction to produce COFs used as cathodes in lithium-sulphur battery.[149] Not only the dynamic character of this S_NAr reaction was necessary for the synthesis of the material, but the resulting thianthrene units were shown to react in sulphur-sulphur exchange reactions in a post-functionalization strategy. This sulfurization afforded a more stable network showing high performances in batteries, with low loss of capacity after 500 cycles and a current density of 500 mA/g. If this S_NAr reaction involving thiol happens in a dynamic fashion, it is seemingly not the case for analogous dioxin motifs which were prepared employing catechol-based oxygenated nucleophiles.[150] It must be highlighted that oxygen-based nucleophiles were later successfully employed in dynamic S_NAr reactions. In 2022, Zhang and co-workers reported the synthesis of COFs by reversible S_NAr between cyanurate electrophiles and phenol derivatives.[151] This reaction leads to stable and crystalline COFs, however their optoelectronic properties were not investigated. Overall, the use of dynamic S_NAr reactions seem highly promising for the synthesis of ladder-like conjugated materials, but these kinds of reactions remains so far underexploited.

6. Summary and Outlook

DCC and DCBs have been employed to design a variety of opto-electroactive materials mostly following two strategies. The first one is to exploit the self-assembly properties of DCBs to spatially organize π-conjugated units along a template or on a surface. This method affords multidimensional architectures from which new optoelectronic properties emerge. This approach is inspired by the elegantly organized chromophores in biological photosystems. The second approach is to directly connect π-conjugated motifs by DCBs. In this case, depending on the type of structure and the stability of the DCB, which could be more or less dynamic or kinetically inert, conjugated materials are obtained. Some conditions exerted on the final materials, *i.e.* moisture, acids, bases, or strong nucleophiles, can shift the equilibrium of the DCB, and therefore, drastically affect its structure, and potentially alter or destroy its performances. Although this instability is a drawback for the performances of the optoelectronic devices, it can be exploited for recycling the conjugated materials. Overall, DCC is a powerful approach and synthetic tool to create unique optoelectronic materials with remarkable properties, including stimuli-responsiveness. Nonetheless, most of DCBs are poorly conjugated, which limit the electronic conjugation of the final material, and thus, the macroscopic electronic properties.

Knowing these weaknesses, there is a need for dynamic covalent synthetic approaches that can bring together π-conjugated architectures in a precise manner, and at that same time afford stable materials of high performances. One way to alleviate the problem associated with the dynamicity of DCBs is to lock the products in order to isolate and characterize them. This solution has been extensively explored in the synthesis of COFs and applied to the stabilization of self-assembled porous organic cages.[152] The chemical transformation of imines into other functional groups, however, requires the addition of non-innocent chemical reactants which are not compatible with every other functional groups. Furthermore, some of these chemical transformations also lead to even less or not conjugated bridges. Hence, most of the strategies reported so far are facing this dilemma.

As a perspective, we can envision two future directions for the field. First, the self-correcting and adapting behavior of DCBs-based systems deserves to be integrated in more optoelectronic devices. Changing the composition of a dynamic system made of multiple components in exchange, resulting in a response manifested by a change of optical (color) or charge transport (current) properties, is a powerful strategy. We can imagine to exploit this for the design of new (bio)sensors, color-changing OLEDs, self-repairing electronics, energy storage, and more. Secondly, chemists should aim at developing post-synthetic locking strategies that strengthen or at least maintain the electronic conjugation between π-conjugated building blocks. These post-synthetic locking strategies could open up new opportunities for the design of organic semiconductors. These chemical transformations are particularly attracting considering that the reaction involved in dynamic covalent syntheses are often carried out in mild conditions, can be performed with a high atom economy, and in their vast majority, do not require the use of toxic or precious and expensive metal catalysts. Thus, novel organic semiconducting materials based on DCBs have the potential to afford more sustainable organic electronic devices while alleviating part of the synthetic complexity often associated to their preparations. As the interest in both DCC and organic semiconductors have been increasingly growing the past decades, we can be optimistic to see such methodology to emerge in the future.

Acknowledgements

The authors acknowledge the Université d'Angers and SFR MATRIX. This work received support from the "Étoiles Montantes" funding scheme (A. Goujon, project CURVY, 2021_11614, fellowship for A. H. G. David) funded by the PULSAR 2021 program from the Région Pays de la Loire and the Université d'Angers, and the Agence Nationale de la Recherche (A. Goujon, PhotoSynth ANR JCJC 2021, ANR-21-CE06-0015-01, fellowship to A. Gapin and E. Chatir). This work is funded by the European Union (ERC Starting Grant, PhotoFreeze, project n°101116355). A. Goujon warmly acknowledges the bureau of the Organic Chemistry Division of the French Chemical Society (DCO SCF) for the "Marc Julia" Emergent Scientist Award 2023 and the invitation to contribute to this special issue of the European Journal of Organic Chemistry.

Keywords: Dynamic Covalent Chemistry • Organic Materials • Conjugated Systems • Synthetic Chemistry • Organic Electronics

References

[1] P. T. Corbett, J. Leclaire, L. Vial, K. R. West, J.-L. Wietor, J. K. M. Sanders, S. Otto, *Chem. Rev.* **2006**, *106*, 3652–3711.
[2] W. Zhang, Y. Jin, Eds. *Dynamic Covalent Chemistry: Principles, Reactions, and Applications*, J. Wiley And Sons, Ltd., London, **2017**.
[3] Y. Jin, C. Yu, R. J. Denman, W. Zhang, *Chem. Soc. Rev.* **2013**, *42*, 6634–6654.
[4] S. J. Rowan, S. J. Cantrill, G. R. L. Cousins, J. K. M. Sanders, J. F. Stoddart, *Angew. Chem. Int. Ed.* **2002**, *41*, 898–952.
[5] T. Santos, D. S. Rivero, Y. Pérez-Pérez, E. Martín-Encinas, J. Pasán, A. H. Daranas, R. Carrillo, *Angew. Chem. Int. Ed.* **2021**, *60*, 18783–18791.
[6] J. Li, P. Nowak, S. Otto, *J. Am. Chem. Soc.* **2013**, *135*, 9222–9239.
[7] M. Mondal, A. K. H. Hirsch, *Chem. Soc. Rev.* **2015**, *44*, 2455–2488.
[8] F. B. L. Cougnon, J. K. M. Sanders, *Acc. Chem. Res.* **2012**, *45*, 2211–2221.
[9] A. Wilson, G. Gasparini, S. Matile, *Chem. Soc. Rev.* **2014**, *43*, 1948–1962.
[10] S. Lascano, K.-D. Zhang, R. Wehlauch, K. Gademann, N. Sakai, S. Matile, *Chem. Sci.* **2016**, *7*, 4720–4724.
[11] Z. Rodriguez-Docampo, S. Otto, *Chem. Commun.* **2008**, 5301–5303.
[12] S. Erbas-Cakmak, S. D. P. Fielden, U. Karaca, D. A. Leigh, C. T. McTernan, D. J. Tetlow, M. R. Wilson, *Science* **2017**, *358*, 340–343.
[13] N. Zheng, Y. Xu, Q. Zhao, T. Xie, *Chem. Rev.* **2021**, *121*, 1716–1745.
[14] E. Moulin, G. Cormos, N. Giuseppone, *Chem. Soc. Rev.* **2012**, *41*, 1031–1049.
[15] S. Wang, M. W. Urban, *Nat. Rev. Mater.* **2020**, *5*, 562–583.
[16] F. B. L. Cougnon, A. R. Stefankiewicz, S. Ulrich, *Chem. Sci.* **2024**, *15*, 879–895.
[17] H. Bronstein, C. B. Nielsen, B. C. Schroeder, I. McCulloch, *Nat. Rev. Chem.* **2020**, *4*, 66–77.
[18] J. Hu, S. K. Gupta, J. Ozdemir, H. Beyzavi, *ACS Appl. Nano Mater.* **2020**, *3*, 6239–6269.
[19] O. Kulyk, L. Rocard, L. Maggini, D. Bonifazi, *Chem. Soc. Rev.* **2020**, *49*, 8400–8424.
[20] R. Bhosale, J. Míšek, N. Sakai, S. Matile, *Chem. Soc. Rev.* **2009**, *39*, 138–149.
[21] L. Rocard, A. Berezin, F. De Leo, D. Bonifazi, *Angew. Chem. Int. Ed.* **2015**, *54*, 15739–15743.
[22] N. Sakai, M. Lista, O. Kel, S. Sakurai, D. Emery, J. Mareda, E. Vauthey, S. Matile, *J. Am. Chem. Soc.* **2011**, *133*, 15224–15227.
[23] H. Hayashi, A. Sobczuk, A. Bolag, N. Sakai, S. Matile, *Chem. Sci.* **2014**, *5*, 4610–4614.
[24] J. López-Andarias, A. Bolag, C. Nançoz, E. Vauthey, C. Atienza, N. Sakai, N. Martín, S. Matile, *Chem. Commun.* **2015**, *51*, 7543–7545.

[25] G. Sforazzini, E. Orentas, A. Bolag, N. Sakai, S. Matile, *J. Am. Chem. Soc.* **2013**, *135*, 12082–12090.
[26] H. Schiff, *Liebigs Ann. Chem.* **1864**, *131*, 118–119.
[27] M. E. Belowich, J. F. Stoddart, *Chem. Soc. Rev.* **2012**, *41*, 2003–2024.
[28] C. D. Meyer, C. S. Joiner, J. F. Stoddart, *Chem. Soc. Rev.* **2007**, *36*, 1705–1723.
[29] K.-D. Kreuer, S. J. Paddison, E. Spohr, M. Schuster, *Chem. Rev.* **2004**, *104*, 4637–4678.
[30] J. Rivnay, S. Inal, A. Salleo, R. M. Owens, M. Berggren, G. G. Malliaras, *Nat. Rev. Mater.* **2018**, *3*, 17086.
[31] P. Wei, Y. Sui, X. Meng, Q. Zhou, *J. App. Polym. Sci.* **2023**, *140*, e53919.
[32] X. Meng, H.-N. Wang, S.-Y. Song, H.-J. Zhang, *Chem. Soc. Rev.* **2017**, *46*, 464–480.
[33] Z. Heravifard, A. R. Akbarzadeh, L. Tayebi, R. Rahimi, *ChemistrySelect* **2022**, *7*, e202202005.
[34] M. J. Strauss, M. Jia, A. M. Evans, I. Castano, R. L. Li, X. Aguilar-Enriquez, E. K. Roesner, J. L. Swartz, A. D. Chavez, A. E. Enciso, J. F. Stoddart, M. Rolandi, W. R. Dichtel, *J. Am. Chem. Soc.* **2021**, *143*, 8145–8153.
[35] X. Yang, Z. Ullah, J. F. Stoddart, C. T. Yavuz, *Chem. Rev.* **2023**, *123*, 4602–4634.
[36] M. Liu, L. Chen, S. Lewis, S. Y. Chong, M. A. Little, T. Hasell, I. M. Aldous, C. M. Brown, M. W. Smith, C. A. Morrison, L. J. Hardwick, A. I. Cooper, *Nat. Commun.* **2016**, *7*, 12750.
[37] D.-W. Lim, H. Kitagawa, *Chem. Rev.* **2020**, *120*, 8416–8467.
[38] R. Han, P. Wu, *ACS Appl. Mater. Interfaces* **2018**, *10*, 18351–18358.
[39] X. Xu, Z. Shao, L. Shi, B. Cheng, X. Yin, X. Zhuang, Y. Di, *Polym. Adv. Technol.* **2020**, *31*, 1571–1580.
[40] X. Zheng, W. Zhu, C. Zhang, Y. Zhang, C. Zhong, H. Li, G. Xie, X. Wang, C. Yang, *J. Am. Chem. Soc.* **2019**, *141*, 4704–4710.
[41] H.-T. Feng, Y.-X. Yuan, J.-B. Xiong, Y.-S. Zheng, B. Z. Tang, *Chem. Soc. Rev.* **2018**, *47*, 7452–7476.
[42] M. Taghi Sharbati, M. N. Soltani Rad, S. Behrouz, A. Gharavi, F. Emami, *J. Lumin.* **2011**, *131*, 553–558.
[43] J. Li, J. Qi, F. Jin, F. Zhang, L. Zheng, L. Tang, R. Huang, J. Xu, H. Chen, M. Liu, Y. Qiu, A. I. Cooper, Y. Shen, L. Chen, *Nat. Commun.* **2022**, *13*, 2031.
[44] L. Zhang, Y. Jia, F. Meng, L. Sun, F. Cheng, Z. Shi, R. Jiang, X. Song, *J. Alloys Compd.* **2022**, *923*, 166488.
[45] S. Sharma, G. A. Andrade, S. Maurya, I. A. Popov, E. R. Batista, B. L. Davis, R. Mukundan, N. C. Smythe, A. M. Tondreau, P. Yang, J. C. Gordon, *Energy Storage Mater.* **2021**, *37*, 576–586.
[46] X. Feng, P. Liao, J. Jiang, J. Shi, Z. Ke, J. Zhang, *ChemPhotoChem* **2019**, *3*, 1014–1019.
[47] H.-H. Huang, K. S. Song, A. Prescimone, A. Aster, G. Cohen, R. Mannancherry, E. Vauthey, A. Coskun, T. Šolomek, *Chem. Sci.* **2021**, *12*, 5275–5285.
[48] R. Ham, C. J. Nielsen, S. Pullen, J. N. H. Reek, *Chem. Rev.* **2023**, *123*, 5225–5261.
[49] H.-Y. Lin, L.-Y. Zhou, L. Xu, *Chem. Asian J* **2021**, *16*, 3805–3816.
[50] A. Goujon, L. Rocard, T. Cauchy, P. Hudhomme, *J. Org. Chem.* **2020**, *85*, 7218–7224.
[51] T. Sharma, P. Mahajan, M. Adil Afroz, A. Singh, Yukta, N. Kumar Tailor, S. Purohit, S. Verma, B. Padha, V. Gupta, S. Arya, S. Satapathi, *ChemSusChem* **2022**, *15*, e202101067.
[52] D. Luo, W. Jang, D. D. Babu, M. S. Kim, D. H. Wang, A. K. K. Kyaw, *J. Mater. Chem. A* **2022**, *10*, 3255–3295.
[53] R. El-Berjawi, L. Rocard, A. Goujon, T. Cauchy, P. Hudhomme, *J. Org. Chem.* **2020**, *85*, 12252–12261.
[54] A. Goujon, L. Rocard, H. Melville, T. Cauchy, C. Cabanetos, S. Dabos-Seignon, P. Hudhomme, *J. Mater. Chem. C* **2022**, *10*, 14939–14945.
[55] A. Makhloutah, A. Hoff, A. Goujon, G. C. Welch, P. Hudhomme, *Mater. Chem. Front.* **2022**, *6*, 3237–3242.
[56] A. Gapin, A. H. G. David, M. Allain, D. Masson, O. Aleveque, T. Ave, L. Le Bras, P. Hudhomme, A. Goujon, *Chem. Eur. J.* **2023**, 29, e202300652.
[57] A. H. G. David, D. Shymon, H. Melville, L.-A. Accou, A. Gapin, M. Allain, O. Alévêque, M. Force, A. Grosjean, P. Hudhomme, L. L. Bras, A. Goujon, *J. Mater. Chem. C* **2023**, *11*, 14631–14640.
[58] T. P. King, S. W. Zhao, T. Lam, *Biochemistry* **1986**, *25*, 5774–5779.
[59] A. Dirksen, S. Yegneswaran, P. E. Dawson, *Angew. Chem. Int. Ed.* **2010**, *49*, 2023–2027.
[60] F. della Sala, E. R. Kay, *Angew. Chem. Int. Ed.* **2015**, *54*, 4187–4191.
[61] Y. Hu, J. Li, Y. Zhou, J. Shi, G. Li, H. Song, Y. Yang, J. Shi, W. Hong, *Angew. Chem. Int. Ed.* **2021**, *60*, 20872–20878.
[62] B.-P. Cao, C. Dai, X. Wang, Q. Xiao, D. Wei, *Sensors* **2022**, *22*, 6947.
[63] R. Singh, G. M. Whitesides, in *The Chemistry of Sulfur-Containing Functional Groups*, J. Wiley And Sons, Ltd., London, **1993**, pp. 633–658.
[64] E.-K. Bang, M. Lista, G. Sforazzini, N. Sakai, S. Matile, *Chem. Sci.* **2012**, *3*, 1752–1763.
[65] R. Zhang, T. Nie, Y. Fang, H. Huang, J. Wu, *Biomacromolecules* **2022**, *23*, 1–19.
[66] N. J. Bulleid, L. Ellgaard, *Trends Biochem. Sci.* **2011**, *36*, 485–492.
[67] N. E. Zhou, C. M. Kay, R. S. Hodges, *Biochemistry* **1993**, *32*, 3178–3187.
[68] C. S. Sevier, C. A. Kaiser, *Nat. Rev. Mol. Cell. Biol.* **2002**, *3*, 836–847.
[69] S. P. Black, J. K. M. Sanders, A. R. Stefankiewicz, *Chem. Soc. Rev.* **2014**, *43*, 1861–1872.
[70] N. Ponnuswamy, F. B. L. Cougnon, J. M. Clough, G. D. Pantoş, J. K. M. Sanders, *Science* **2012**, *338*, 783–785.
[71] M. H. Lee, Z. Yang, C. W. Lim, Y. H. Lee, S. Dongbang, C. Kang, J. S. Kim, *Chem. Rev.* **2013**, *113*, 5071–5109.
[72] Y. He, Z. Chang, S. Wu, H. Zhou, *J. Mater. Chem. A* **2018**, *6*, 6155–6182.
[73] Y.-X. Yin, S. Xin, Y.-G. Guo, L.-J. Wan, *Angew. Chem. Int. Ed.* **2013**, *52*, 13186–13200.
[74] M. Zhao, B.-Q. Li, X.-Q. Zhang, J.-Q. Huang, Q. Zhang, *ACS Cent. Sci.* **2020**, *6*, 1095–1104.
[75] P. Sang, Q. Chen, D.-Y. Wang, W. Guo, Y. Fu, *Chem. Rev.* **2023**, *123*, 1262–1326.
[76] A. Bhargav, Y. Ma, K. Shashikala, Y. Cui, Y. Losovyj, Y. Fu, *J. Mater. Chem. A* **2017**, *5*, 25005–25013.
77] F. Li, Y. Si, B. Liu, Z. Li, Y. Fu, *Adv. Funct. Mater.* **2019**, *29*, 1902223.
[78] M. Wu, Y. Cui, A. Bhargav, Y. Losovyj, A. Siegel, M. Agarwal, Y. Ma, Y. Fu, *Angew. Chem. Int. Ed.* **2016**, *55*, 10027–10031.
[79] J. Song, Y. Si, W. Guo, D. Wang, Y. Fu, *Angew. Chem. Int. Ed.* **2021**, *133*, 9969–9973.
[80] H. Yang, X. Li, Y. Wang, L. Gao, J. Li, D. Zhang, T. Lin, *J. Power Sources* **2020**, *452*, 227785.
[81] S. Ji, J. Xia, H. Xu, *ACS Macro Lett.* **2016**, *5*, 78–82.
[82] C. Liu, J. Xia, S. Ji, Z. Fan, H. Xu, *Chem. Commun.* **2019**, *55*, 2813–2816.
[83] J. Zhao, Y. Si, Z. Han, J. Li, W. Guo, Y. Fu, *Angew. Chem. Int. Ed.* **2020**, *59*, 2654–2658.
[84] J. Zhao, W. Guo, Y. Fu, *Mater. Today Energy* **2020**, *17*, 100442.
[85] W. Guo, A. Bhargav, J. D. Ackerson, Y. Cui, Y. Ma, Y. Fu, *Chem. Commun.* **2018**, *54*, 8873–8876.
[86] Q. Chen, Y. Si, W. Guo, Y. Fu, *Chem. Commun.* **2022**, *58*, 10993–10996.
[87] W. Zhang, F. Ma, Q. Wu, Z. Zeng, W. Zhong, S. Cheng, X. Chen, J. Xie, *Energy Environ. Mater.* **2023**, *6*, e12369.
[88] S. Lee, A. Yang, T. P. I. Moneypenny, J. S. Moore, *J. Am. Chem. Soc.* **2016**, *138*, 2182–2185.
[89] A. Fürstner, *Angew. Chem. Int. Ed.* **2013**, *52*, 2794–2819.
[90] A. Petronico, T. P. I. Moneypenny, B. G. Nicolau, J. S. Moore, R. G. Nuzzo, A. A. Gewirth, *J. Am. Chem. Soc.* **2018**, *140*, 7504–7509.
[91] Y. Yi, H. Xu, L. Wang, W. Cao, X. Zhang, *Chem. Eur. J.* **2013**, *19*, 9506–9510.
[92] N. Zheng, Y. Feng, Y. Zhang, R. Li, C. Bian, L. Bao, S. Du, H. Dong, Y. Shen, W. Feng, *ACS Appl. Mater. Interfaces* **2019**, *11*, 24360–24366.
[93] T. M. FitzSimons, E. V. Anslyn, A. M. Rosales, *ACS Polym. Au* **2022**, *2*, 129–136.
[94] N. Kuhl, R. Geitner, R. K. Bose, S. Bode, B. Dietzek, M. Schmitt, J. Popp, S. J. Garcia, S. van der Zwaag, U. S. Schubert, M. D. Hager, *Macromol. Chem. Phys.* **2016**, *217*, 2541–2550.
[95] R. Baruah, A. Kumar, R. R. Ujjwal, S. Kedia, A. Ranjan, U. Ojha, *Macromolecules* **2016**, *49*, 7814–7824.
[96] P. A. Jackson, J. C. Widen, D. A. Harki, K. M. Brummond, *J. Med. Chem.* **2017**, *60*, 839–885.
[97] H. Liu, S. Wang, H. Gao, Z. Shen, *Eur. J. Org. Chem.* **2020**, *2020*, 5647–5663.
[98] Z. Liu, X. Zhou, Y. Miao, Y. Hu, N. Kwon, X. Wu, J. Yoon, *Angew. Chem. Int. Ed.* **2017**, *56*, 5812–5816.
[99] F. García, M. M. J. Smulders, *J. Polym. Sci., Part A: Polym. Chem.* **2016**, *54*, 3551–3577.
[100] S. Huang, X. Kong, Y. Xiong, X. Zhang, H. Chen, W. Jiang, Y. Niu, W. Xu, C. Ren, *Eur. Polym. J.* **2020**, *141*, 110094.
[101] L. Ding, Z.-D. Yu, X.-Y. Wang, Z.-F. Yao, Y. Lu, C.-Y. Yang, J.-Y. Wang, J. Pei, *Chem. Rev.* **2023**, *123*, 7421–7497.
[102] N. Sakai, S. Matile, *J. Am. Chem. Soc.* **2018**, *140*, 11438–11443.
[103] D. Schultz, F. Biaso, A. R. M. Shahi, M. Geoffroy, K. Rissanen, L. Gagliardi, C. J. Cramer, J. R. Nitschke, *Chem. Eur. J.* **2008**, *14*, 7180–7185.
[104] J. L. Greenfield, F. J. Rizzuto, I. Goldberga, J. R. Nitschke, *Angew. Chem. Int. Ed.* **2017**, *56*, 7541–7545.
[105] J. L. Greenfield, D. Di Nuzzo, E. W. Evans, S. P. Senanayak, S. Schott, J. T. Deacon, A. Peugeot, W. K. Myers, H. Sirringhaus, R. H. Friend, J. R. Nitschke, *Adv. Mater.* **2021**, *33*, 2100403.
[106] X. de Hatten, D. Asil, R. H. Friend, J. R. Nitschke, *J. Am. Chem. Soc.* **2012**, *134*, 19170–19178.
[107] A.-E. Dascalu, L. Halgreen, A. Torres-Huerta, H. Valkenier, *Chem. Commun.* **2022**, *58*, 11103–11106.
[108] W. Hong, B. Sun, H. Aziz, W.-T. Park, Y.-Y. Noh, Y. Li, *Chem. Commun.* **2012**, *48*, 8413.
[109] G. Wang, P. Kumar, Z. Zhang, A. D. Hendsbee, H. Liu, X. Li, J. Wang, Y. Li, *RSC Advances* **2020**, *10*, 12876–12882.
[110] H. Murakami, K. Kobayashi, K. Suzuki, T. Yasuda, T. Kanbara, J. Kuwabara, *Macromolecules* **2021**, *54*, 11281–11288.
[111] Y. Zhang, Y. Lang, G. Li, *EcoMat* **2023**, *5*, e12281.
[112] F. Torricelli, I. Alessandri, E. Macchia, I. Vassalini, M. Maddaloni, L. Torsi, *Adv. Mater. Technol.* **2022**, *7*, 2100445.
[113] T. Lei, M. Guan, J. Liu, H.-C. Lin, R. Pfattner, L. Shaw, A. F. McGuire, T.-C. Huang, L. Shao, K.-T. Cheng, J. B.-H. Tok, Z. Bao, *Proc. Natl. Acad. Sci. U. S. A.* **2017**, *114*, 5107–5112.
[114] H. Tran, V. R. Feig, K. Liu, H.-C. Wu, R. Chen, J. Xu, K. Deisseroth, Z. Bao, *ACS Cent. Sci.* **2019**, *5*, 1884–1891.
[115] A. Uva, A. Lin, H. Tran, *J. Am. Chem. Soc.* **2023**, *145*, 3606–3614.

[116] W. Hong, C. Guo, B. Sun, Y. Li, *J. Mater. Chem. C* **2015**, *3*, 4464–4470.
[117] H. Tran, S. Nikzad, J. A. Chiong, N. J. Schuster, A. E. Peña-Alcántara, V. R. Feig, Y.-Q. Zheng, Z. Bao, *Chem. Mater.* **2021**, *33*, 7465–7474.
[118] K. Hu, H. Yang, W. Zhang, Y. Qin, *Chem. Sci.* **2013**, *4*, 3649–3653.
[119] A. M. Evans, M. J. Strauss, A. R. Corcos, Z. Hirani, W. Ji, L. S. Hamachi, X. Aguilar-Enriquez, A. D. Chavez, B. J. Smith, W. R. Dichtel, *Chem. Rev.* **2022**, *122*, 442–564.
[120] H. M. El-Kaderi, J. R. Hunt, J. L. Mendoza-Cortés, A. P. Côté, R. E. Taylor, M. O'Keeffe, O. M. Yaghi, *Science* **2007**, *316*, 268–272.
[121] P. J. Waller, F. Gándara, O. M. Yaghi, *Acc. Chem. Res.* **2015**, *48*, 3053–3063.
[122] R. K. Sharma, P. Yadav, M. Yadav, R. Gupta, P. Rana, A. Srivastava, R. Zbořil, R. S. Varma, M. Antonietti, M. B. Gawande, *Mater. Horiz.* **2020**, *7*, 411–454.
[123] T. Zhang, G. Zhang, L. Chen, *Acc. Chem. Res.* **2022**, *55*, 795–808.
[124] X. Guan, F. Chen, Q. Fang, S. Qiu, *Chem. Soc. Rev.* **2020**, *49*, 1357–1384.
[125] Y. Yang, K. Börjesson, *Trends Chem.* **2022**, *4*, 60–75.
[126] H. Chen, H. S. Jena, X. Feng, K. Leus, P. Van Der Voort, *Angew. Chem. Int. Ed.* **2022**, *61*, e202204938.
[127] D. D. Medina, T. Sick, T. Bein, *Adv. Energy Mater.* **2017**, *7*, 1700387.
[128] Y. Li, Q. Chen, T. Xu, Z. Xie, J. Liu, X. Yu, S. Ma, T. Qin, L. Chen, *J. Am. Chem. Soc.* **2019**, *141*, 13822–13828.
[129] C. Wu, Y. Liu, H. Liu, C. Duan, Q. Pan, J. Zhu, F. Hu, X. Ma, T. Jiu, Z. Li, Y. Zhao, *J. Am. Chem. Soc.* **2018**, *140*, 10016–10024.
[130] S. Wan, F. Gándara, A. Asano, H. Furukawa, A. Saeki, S. K. Dey, L. Liao, M. W. Ambrogio, Y. Y. Botros, X. Duan, S. Seki, J. F. Stoddart, O. M. Yaghi, *Chem. Mater.* **2011**, *23*, 4094–4097.
[131] S. Fu, E. Jin, H. Hanayama, W. Zheng, H. Zhang, L. Di Virgilio, M. A. Addicoat, M. Mezger, A. Narita, M. Bonn, K. Müllen, H. I. Wang, *J. Am. Chem. Soc.* **2022**, *144*, 7489–7496.
[132] S. Kim, H. Lim, J. Lee, H. C. Choi, *Langmuir* **2018**, *34*, 8731–8738.
[133] Y. Li, M. Liu, J. Wu, J. Li, X. Yu, Q. Zhang, *Front. Optoelectron.* **2022**, *15*, 38.
[134] L. Cusin, H. Peng, A. Ciesielski, P. Samorì, *Angew. Chem. Int. Ed.* **2021**, *60*, 14236–14250.
[135] X. Huang, C. Sun, X. Feng, *Sci. China Chem.* **2020**, *63*, 1367–1390.
[136] C. Mo, M. Yang, F. Sun, J. Jian, L. Zhong, Z. Fang, J. Feng, D. Yu, *Adv. Sci.* **2020**, *7*, 1902988.
[137] G. Fu, D. Yang, S. Xu, S. Li, Y. Zhao, H. Yang, D. Wu, P. S. Petkov, Z.-A. Lan, X. Wang, T. Zhang, *J. Am. Chem. Soc.* **2024**, *146*, 1318–1325.
[138] S. Kandambeth, A. Mallick, B. Lukose, M. V. Mane, T. Heine, R. Banerjee, *J. Am. Chem. Soc.* **2012**, *134*, 19524–19527.
[139] X. Li, C. Zhang, S. Cai, X. Lei, V. Altoe, F. Hong, J. J. Urban, J. Ciston, E. M. Chan, Y. Liu, *Nat. Commun.* **2018**, *9*, 2998.
[140] S. J. Lyle, T. M. Osborn Popp, P. J. Waller, X. Pei, J. A. Reimer, O. M. Yaghi, *J. Am. Chem. Soc.* **2019**, *141*, 11253–11258.
[141] Y. Li, W. Chen, G. Xing, D. Jiang, L. Chen, *Chem. Soc. Rev.* **2020**, *49*, 2852–2868.
[142] W. J. Ong, T. M. Swager, *Nat. Chem.* **2018**, *10*, 1023–1030.
[143] P. J. Waller, S. J. Lyle, T. M. Osborn Popp, C. S. Diercks, J. A. Reimer, O. M. Yaghi, *J. Am. Chem. Soc.* **2016**, *138*, 15519–15522.
[144] H. Liu, J. Chu, Z. Yin, X. Cai, L. Zhuang, H. Deng, *Chem* **2018**, *4*, 1696–1709.
[145] F. Haase, B. V. Lotsch, *Chem. Soc. Rev.* **2020**, *49*, 8469–8500.
[146] G. Jiang, W. Zou, Z. Ou, W. Zhang, Z. Liang, L. Du, *Chem. Eur. J.* **2023**, *29*, e202203610.
[147] Z. Miao, T. Quainoo, T. M. Czyszczon-Burton, N. Rotthowe, J. M. Parr, Z.-F. Liu, M. S. Inkpen, *Nano Lett.* **2022**, *22*, 8331–8338.
[148] Y. Hu, C. Wu, Q. Pan, Y. Jin, R. Lyu, V. Martinez, S. Huang, J. Wu, L. J. Wayment, N. A. Clark, M. B. Raschke, Y. Zhao, W. Zhang, *Nat. Synth.* **2022**, *1*, 449–454.
[149] S. Haldar, M. Wang, P. Bhauriyal, A. Hazra, A. H. Khan, V. Bon, M. A. Isaacs, A. De, L. Shupletsov, T. Boenke, J. Grothe, T. Heine, E. Brunner, X. Feng, R. Dong, A. Schneemann, S. Kaskel, *J. Am. Chem. Soc.* **2022**, *144*, 9101–9112.
[150] B. Zhang, M. Wei, H. Mao, X. Pei, S. A. Alshmimri, J. A. Reimer, O. M. Yaghi, *J. Am. Chem. Soc.* **2018**, *140*, 12715–12719.
[151] Z. Lei, L. J. Wayment, J. R. Cahn, H. Chen, S. Huang, X. Wang, Y. Jin, S. Sharma, W. Zhang, *J. Am. Chem. Soc.* **2022**, *144*, 17737–17742.
[152] H. Wang, Y. Jin, N. Sun, W. Zhang, J. Jiang, *Chem. Soc. Rev.* **2021**, *50*, 8874–8886.

10.1002/ejoc.202400211

WILEY VCH

REVIEW

Entry for the Table of Contents

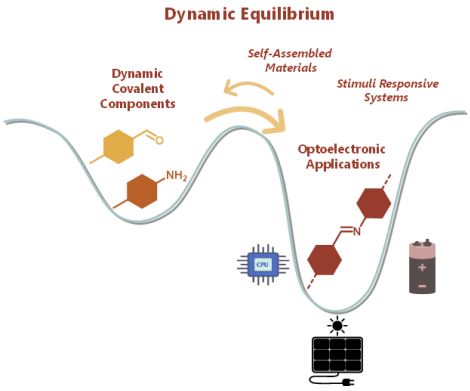

Dynamic Covalent Chemistry can bring together simple components to create complex self-assembled materials. This strategy is so far under-investigated in the field of optoelectronic and energy materials. However, it has the potential to rapidly produce self-assembled organic semiconductors or stimuli responsive devices. Herein, we highlight the advantages of the dynamic covalent approaches and their limitations when applied to this field.

Institute and/or researcher Twitter usernames: @antoinegoujon1, @elarbichatir, @arthurhgdavid, @adelegapin, @moltech_anjou, @univangers, @eurlumomat